

**Active crystallization from power functional theory**Sophie Hermann \* and Matthias Schmidt †*Theoretische Physik II, Physikalisches Institut, Universität Bayreuth, D-95447 Bayreuth, Germany* (Received 21 August 2023; accepted 6 February 2024; published 23 February 2024)

We address the gas, liquid, and crystal phase behaviors of active Brownian particles in three dimensions. The nonequilibrium force balance at coexistence leads to equality of state functions for which we use power functional approximations. Motility-induced phase separation starts at a critical point and quickly becomes metastable against active freezing for Péclet numbers above a nonequilibrium triple point. The mean swim speed acts as a state variable, similar to the density of depletion agents in colloidal demixing. We obtain agreement with recent simulation results and correctly predict the strength of particle number fluctuations in active fluids.

DOI: [10.1103/PhysRevE.109.L022601](https://doi.org/10.1103/PhysRevE.109.L022601)

The occurrence of freezing in a many-body system is often due to the presence of strong, short-ranged repulsion between the constituent particles [1,2]. Conditions of high enough density are required for crystallization as a global ordering phenomenon to occur and these can be induced by external constraints, such as confinement by walls or via interparticle attraction [3,4]. In colloidal systems, attraction between the particles can be generated by adding depletion agents, such as polymers, colloidal rods, or smaller-sized colloidal spheres. The depletants create an effective attraction between the primary particles and the resulting effective interaction potential is accessible via formally integrating out (averaging over) the depletant degrees of freedom [5–11] and via recent machine learning [12,13]. In general, the resulting interaction potential has a strong many-body character, although notable exceptions exist, such as the Asakura-Oosawa model [7,8,10,11], where for sufficiently small polymer-to-colloid size ratio a description based on an effective pair potential is exact [7].

In a striking analogy, Turci and Wilding [14] recently related the phase behavior of three-dimensional active Brownian particles (ABPs) [14,15] to such depletion-driven binary mixtures. ABPs form a central model system for active matter and their phase behavior has received much prior attention [16–22], including the two-dimensional version of the model [16,21,22]. The particles undergo overdamped Brownian motion and they self-propel (swim) along a built-in direction, which diffuses freely. The system displays motility-induced phase separation (MIPS) into dense and dilute coexisting nonequilibrium steady states, despite the absence of explicit interparticle attraction. The phenomenon was addressed on the basis of a wide variety of theoretical techniques [19–23], including recent work by Omar *et al.* [24] based on forces. However, none of these approaches has yet been applied to active freezing.

Despite the significant number of theoretical efforts [19–25], no consensus has been reached on a common

framework which would act as an uncontested platform for the description of active systems, such as the theory of simple liquids for spatially inhomogeneous and phase-separated systems in equilibrium [1,26–28]. It is a rather common point of view that “the link between experiment and theory in active matter is often rather qualitative” [29]. Having a predictive theory is highly valuable though, given that much relevant experimental work is being carried out, e.g., based on light-controlled systems [30], as also used in studies of active polarization [31,32], cluster formation [33], the self-propulsion mechanism of Quincke rollers [29], the experimental study of active sedimentation [34], capillary rise [35], and polycrystallinity [36]. Equally so, simulation studies of wetting [37], vortex crystal formation [38], inertial effects in nematic turbulence [39], interfacial properties [40], and dynamical features [41] of active particles could benefit from having a predictive theory.

In this Letter, we use power functional theory [42], which is a general framework for the description of the dynamics of many-body systems, including ABPs [42–47]. We base our treatment of freezing on the active force balance, as used in studies of active drag forces [43,44], MIPS [45,46], and the interfacial tension between phase-separated states [47] in two-dimensional ABPs. The theory satisfies exact sum rules which result from Noether’s theorem for correlation functions [48,49] as well as from the continuity equation for the global polarization [50]. We demonstrate that the framework gives a physically sound and quantitatively reasonable account of the full phase behavior of ABPs in three dimensions. In their analogy, Turci and Wilding [14] suggested that the Péclet number, which measures the strength of the self-propulsion in the active system relative to diffusive motion, is akin to the depletants’ fugacity (or polymer reservoir density) in an equilibrium mixture. We confirm and extend this point of view, as in our theoretical approach, the mean swim speed plays a role akin to the actual polymer density in the colloid-polymer mixture.

We work on the level of one-body correlation functions, which depend on position  $\mathbf{r}$  and on particle orientation, as represented by a unit vector  $\boldsymbol{\omega}$ . The continuity equation relates

\*Sophie.Hermann@uni-bayreuth.de

†Matthias.Schmidt@uni-bayreuth.de

the divergence of the translational current  $\mathbf{J}(\mathbf{r}, \boldsymbol{\omega}, t)$  and of the rotational current  $\mathbf{J}^\omega(\mathbf{r}, \boldsymbol{\omega}, t)$  to temporal changes of the one-body density distribution according to

$$\frac{\partial \rho(\mathbf{r}, \boldsymbol{\omega}, t)}{\partial t} = -\nabla \cdot \mathbf{J}(\mathbf{r}, \boldsymbol{\omega}, t) - \nabla^\omega \cdot \mathbf{J}^\omega(\mathbf{r}, \boldsymbol{\omega}, t). \quad (1)$$

Here  $\nabla$  and  $\nabla^\omega$  indicate the derivatives with respect to  $\mathbf{r}$  and  $\boldsymbol{\omega}$ , respectively, and the density profile  $\rho(\mathbf{r}, \boldsymbol{\omega}, t)$  is position- and orientation-resolved. We consider steady states such that the left-hand side of Eq. (1) vanishes and we drop the time argument  $t$  from here on. As no explicit torques act in the system, the orientational current stems solely from the free rotational diffusion of the active spheres:  $\mathbf{J}^\omega(\mathbf{r}, \boldsymbol{\omega}) = -D_{\text{rot}} \nabla^\omega \rho(\mathbf{r}, \boldsymbol{\omega})$ , where  $D_{\text{rot}}$  indicates the rotational diffusion constant. For the present case of overdamped active motion, the exact force balance is given by

$$\gamma \mathbf{v}(\mathbf{r}, \boldsymbol{\omega}) = \mathbf{f}_{\text{id}}(\mathbf{r}, \boldsymbol{\omega}) + \mathbf{f}_{\text{int}}(\mathbf{r}, \boldsymbol{\omega}) + \gamma s \boldsymbol{\omega}. \quad (2)$$

The left-hand side of Eq. (2) represents the negative friction force with friction constant  $\gamma$  and the velocity field is the ratio of current and density,  $\mathbf{v}(\mathbf{r}, \boldsymbol{\omega}) = \mathbf{J}(\mathbf{r}, \boldsymbol{\omega})/\rho(\mathbf{r}, \boldsymbol{\omega})$ . The three driving contributions on the right-hand side of Eq. (2) are the ideal diffusive force field  $\mathbf{f}_{\text{id}}(\mathbf{r}, \boldsymbol{\omega}) = -k_B T \nabla \ln \rho(\mathbf{r}, \boldsymbol{\omega})$ , the internal force field  $\mathbf{f}_{\text{int}}(\mathbf{r}, \boldsymbol{\omega})$ , which arises from the Weeks-Chandler-Anderson (WCA) interparticle interactions, and the swim force  $\gamma s \boldsymbol{\omega}$  with  $s$  indicating the speed of free swimming. The one-body interparticle interaction force field  $\mathbf{f}_{\text{int}}(\mathbf{r}, \boldsymbol{\omega})$  is accessible via sampling in simulations [43–46] and via machine learning, as recently demonstrated in passive flow [51] and in equilibrium [52,53]. When averaged over orientation  $\boldsymbol{\omega}$ , there is no net flow in the stationary states considered here:  $\int d\boldsymbol{\omega} \mathbf{J}(\mathbf{r}, \boldsymbol{\omega}) = 0$ .

We split the interparticle forces according to [47,54]

$$\mathbf{f}_{\text{int}}(\mathbf{r}, \boldsymbol{\omega}) = \mathbf{f}_{\text{ad}}(\mathbf{r}) + \mathbf{f}_{\text{flow}}(\mathbf{r}, \boldsymbol{\omega}) + \mathbf{f}_{\text{struc}}(\mathbf{r}, \boldsymbol{\omega}), \quad (3)$$

where the right-hand side consists of the adiabatic force field  $\mathbf{f}_{\text{ad}}(\mathbf{r})$ , the superadiabatic flow force field  $\mathbf{f}_{\text{flow}}(\mathbf{r}, \boldsymbol{\omega})$  and the superadiabatic structural force field  $\mathbf{f}_{\text{struc}}(\mathbf{r}, \boldsymbol{\omega})$ . Here the adiabatic force field  $\mathbf{f}_{\text{ad}}(\mathbf{r})$  is defined as acting in an equilibrium system of passive WCA particles that do not swim. The WCA particles are spheres and hence there is no nontrivial dependence on  $\boldsymbol{\omega}$  in the adiabatic system. Its density distribution  $\bar{\rho}(\mathbf{r})$  is identical to the orientation-integrated density distribution in the active system. In the adiabatic system,  $\bar{\rho}(\mathbf{r})$  is stabilized by an external potential.

If one wishes to think in terms of functional dependencies, then  $\mathbf{f}_{\text{ad}}(\mathbf{r})$  is an instantaneous density functional, in the sense of functional dependencies, as they form the core of classical density functional theory of inhomogeneous liquids and solids [1,26–28,42]. Both the flow and the structural force contributions in Eq. (2) are of superadiabatic nature, i.e., they are genuine nonequilibrium force fields which arise from the interparticle interactions [42]. The flow and structural nonequilibrium forces,  $\mathbf{f}_{\text{flow}}(\mathbf{r}, \boldsymbol{\omega})$  and  $\mathbf{f}_{\text{struc}}(\mathbf{r}, \boldsymbol{\omega})$ , have characterizing symmetry properties under motion reversal. Here  $\mathbf{f}_{\text{flow}}(\mathbf{r}, \boldsymbol{\omega})$  changes its sign under sign change of the steady-state velocity profile, while  $\mathbf{f}_{\text{struc}}(\mathbf{r}, \boldsymbol{\omega})$  remains unaffected by the same transformation [42,51,54]. In equilibrium, as well as in passive uniaxial flow, the three force contributions were shown to be amenable to supervised machine

learning [51–53], which we take as confirmation of the general force splitting concept (3), as is here applied to the active system.

The flow force  $\mathbf{f}_{\text{flow}}(\mathbf{r}, \boldsymbol{\omega})$ , as is part of Eq. (3), is defined to compensate the friction and the active force in the force balance relationship (2) such that equality is achieved:

$$\gamma \mathbf{v}(\mathbf{r}, \boldsymbol{\omega}) = \mathbf{f}_{\text{flow}}(\mathbf{r}, \boldsymbol{\omega}) + \gamma s \boldsymbol{\omega}. \quad (4)$$

The flow equation (4) is invariant under motion reversal [42,51,54] and it affects the spatial structure formation as represented by the density profile only indirectly, as we detail below. As an approximation, we resort to the superadiabatic drag force of Ref. [43], which in bulk has the simple form  $\mathbf{f}_{\text{flow}}(\boldsymbol{\omega}) = -\gamma v_b \boldsymbol{\omega} \rho_b / (\rho_j - \rho_b)$ , where  $v_b = \mathbf{v} \cdot \boldsymbol{\omega}$  is the mean forward swim speed [20–23], which is reduced due to particle collisions, when compared to the free swim speed  $s$ . The assumption yields the common linear relationship of the mean swim velocity and the average density,  $v_b/s = 1 - \rho_b/\rho_j$ , independent of position and orientation. The parameter  $\rho_j = \text{const}$ , which we adjust empirically, determines the slope of the decay of  $v_b$  with bulk density and we adjust its value to  $\rho_j = 1.436\sigma^{-3}$ , where  $\sigma$  is the length scale of the WCA pair potential, to approximate the observed behavior [55].

The superadiabatic structural force field  $\mathbf{f}_{\text{sup}}(\mathbf{r}, \boldsymbol{\omega})$  balances the remaining adiabatic and ideal terms in Eq. (2), which implies the following force cancellation:

$$0 = \mathbf{f}_{\text{id}}(\mathbf{r}) + \mathbf{f}_{\text{ad}}(\mathbf{r}) + \mathbf{f}_{\text{struc}}(\mathbf{r}). \quad (5)$$

As a consistency check, the sum of Eqs. (4) and (5) recovers the full force balance relationship (2). The ideal term is generally numerically small, and we hence approximate the exact ideal force  $-k_B T \nabla \ln \rho(\mathbf{r}, \boldsymbol{\omega}) \approx -k_B T \nabla \ln \bar{\rho}(\mathbf{r}) \equiv \mathbf{f}_{\text{id}}(\mathbf{r})$ , where as before  $\bar{\rho}(\mathbf{r})$  is the position-dependent and orientation-averaged one-body density profile. Equation (5) balances the repulsion that acts in the adiabatic system with the nonequilibrium force contributions. We recall that the adiabatic system consists of steeply repulsive spheres without orientations. Hence the structural nonequilibrium forces necessarily need also be independent of orientation,  $\mathbf{f}_{\text{struc}}(\mathbf{r})$ , to satisfy Eq. (5).

As all force fields in Eq. (5) are of gradient nature [the non-gradient forces are contained in Eq. (4)], we can integrate in position and obtain the following chemical potential balance:

$$\mu_{\text{id}}(\mathbf{r}) + \mu_{\text{ad}}(\mathbf{r}) + \mu_{\text{struc}}(\mathbf{r}) = \mu. \quad (6)$$

Here  $\mu = \text{const}$  arises from the spatial integration. All terms on the left-hand side of Eq. (6) are solely defined by generating via spatial differentiation the (negative) force contributions that occur in the structural force balance (5). Explicitly, we have  $\mathbf{f}_{\text{id}}(\mathbf{r}) = -\nabla \mu_{\text{id}}(\mathbf{r})$ , with the standard ideal gas chemical potential expression:  $\mu_{\text{id}}(\mathbf{r}) = -k_B T \ln \bar{\rho}(\mathbf{r})$ ; the adiabatic force field:  $\mathbf{f}_{\text{ad}}(\mathbf{r}) = -\nabla \mu_{\text{ad}}(\mathbf{r})$ ; and the superadiabatic structural force field:  $\mathbf{f}_{\text{struc}}(\mathbf{r}) = -\nabla \mu_{\text{struc}}(\mathbf{r})$ .

Up to having neglected the orientation dependence of the ideal gas contribution and the assumption of the specific simple form of  $\mathbf{f}_{\text{flow}}(\boldsymbol{\omega})$ , the framework thus far developed is exact and we have to resort to approximations to make further progress. We first turn to the adiabatic contribution. The adiabatic state is simply the equilibrium WCA model, which *per se* has no gas-liquid coexistence due to its lack of interparticle

attraction. Treating fluid states of repulsive spheres is straightforward. We approximate the system by hard spheres and use a modified Carnahan-Starling equation of state [56], which correctly accounts for the behavior at very high densities, as is relevant for ABPs in the parameter regime considered here. The corresponding bulk excess free energy  $A_{\text{ad}}$  is given by

$$\frac{A_{\text{ad}}}{Nk_B T} = \frac{3\eta}{1-\eta} + \eta \left\{ (1-\eta) \times \left[ \left( 1 - \eta \left( 1 + \frac{1-\eta_j}{\eta_j} e^{b(\eta-\eta_j)} \right) \right) \right]^{-1} \right\}, \quad (7)$$

where  $\eta = \pi \sigma^3 \rho_b / 6$  is the packing fraction,  $\eta_j = 0.655$  is the densest possible packing fraction in this approximation, and setting  $b = 50$  is an empirical choice [56].

Due to the more complex three-dimensional system, we here choose an advanced approximation for the adiabatic fluid equation of state, as compared to previous work in two dimensions [45–47], where the simple scaled-particle theory was sufficient. An analytical expression for the bulk chemical potential in the adiabatic system then follows from the standard identity  $\mu_{\text{ad}}^b(\rho_b) = [A_{\text{ad}} + \eta \partial A_{\text{ad}} / \partial \eta] / N$ . We use a local density approximation where we evaluate the bulk expression at the value of the local density profile, i.e.,  $\mu_{\text{ad}}(\mathbf{r}) = \mu_{\text{ad}}^b(\bar{\rho}(\mathbf{r}))$ .

To approximate the equation of state of the adiabatic crystal, we resort to the cell theory [57–60]. This yields the chemical potential of the fcc crystal as  $\beta \mu_{\text{cell}} = \ln(\sqrt{2}) + 3 \ln(\Lambda/\sigma) - 3 \ln(\xi - 1) + \xi/(\xi - 1)$ , where  $\xi = [\pi \sqrt{2}/(6\eta)]^{1/3}$  and  $\Lambda$  is the thermal de Broglie wavelength which we set to  $\Lambda = \sigma$ . We only take account of the mean crystal density, and set  $\mu_{\text{ad}} + \mu_{\text{id}} = \mu_{\text{cell}}$  for the treatment of the crystalline phase.

The remaining task is to approximate the superadiabatic structural chemical potential contribution,  $\mu_{\text{struc}}(\mathbf{r})$ . Here we resort to the quiet life approximation, which was successfully used to describe active gas-liquid phase separation in two dimensions, along with the force balance across the free interface between the active bulk states [45,46]. This approximation takes into account, in arguably the simplest correct way, the dependence on both the local density and the local velocity. As the force is structural, it is necessarily even in powers of the velocity. A simple choice which is linear in density and quadratic in velocity [45,46] reads

$$\mu_{\text{struc}}(\mathbf{r}) = \frac{e_1 \gamma}{6D_{\text{rot}}} v^2(\mathbf{r}) \frac{\bar{\rho}(\mathbf{r})}{\rho_j}, \quad (8)$$

where  $e_1 = 0.285$  is a constant that determines the overall strength. This parameter plays the role of a fundamental transport coefficient of the ABP system. Here we fix its value empirically and leave a first-principles derivation to future work. As we also only address bulk states, we set the (squared) local swim velocity to its mean bulk value,  $v^2(\mathbf{r}) = v_b^2$ . Crucially, we use the same approximation (8) for  $\mu_{\text{struc}}$  in all three phases and, in particular, the same value of the constant  $e_1$ .

Nonequilibrium phase coexistence is obtained via the mechanical balance of the total force, which in our framework implies equality of the values of the chemical potential, see Eq. (6), in the coexisting phases, as well as the equality of the pressure. The pressure is obtained from integrating the standard relation  $\rho_b \partial \mu(\rho_b) / \partial \rho_b = \partial P(\rho_b) / \partial \rho_b$ . The resulting

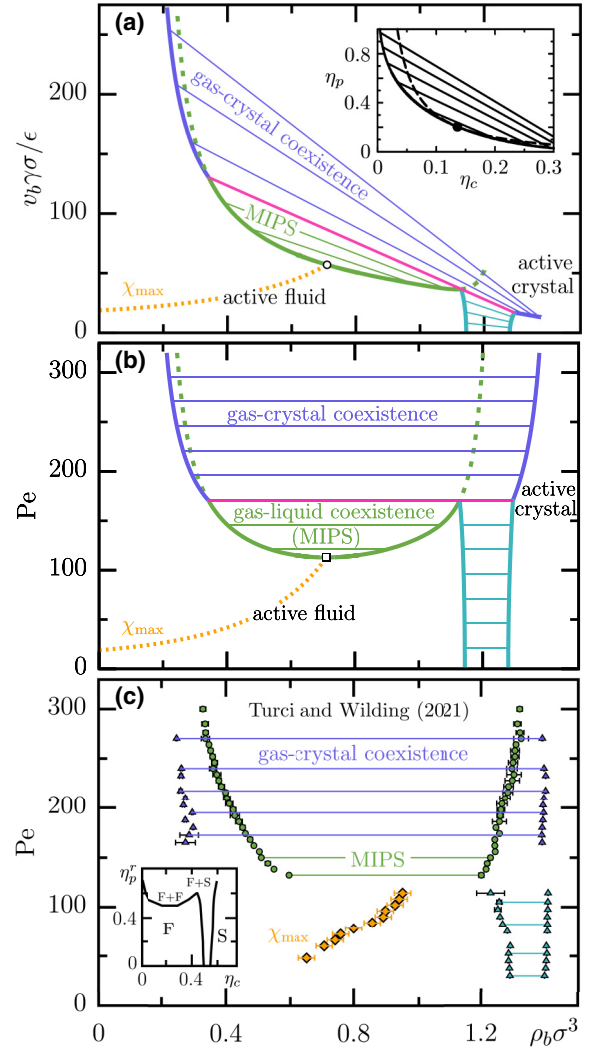


FIG. 1. Phase diagram for three-dimensional ABPs. (a) Theoretical result as a function of the scaled bulk density  $\rho_b \sigma^3$  and the scaled average swim speed  $v_b \gamma \sigma / \epsilon$ . Shown are stable (solid lines) and metastable (dashed lines) binodals; slanted tielines connect coexisting nonequilibrium states. The orange dotted line indicates the line of maximal compressibility  $\chi_{\text{max}}$ . Note the similarity to a phase diagram of a colloid-polymer mixture (inset, adapted from Ref. [8]) as a function of the colloid (polymer) packing fraction  $\eta^c$  ( $\eta^p$ ). (b) Same as (a) but shown as a function of  $\rho_b \sigma^3$  and the Péclet number  $\text{Pe}$ . The tie lines are horizontal in this representation. (c) Same as (b) but obtained from computer simulations in Ref. [14]. Shown are active gas-active fluid (circles) and active gas-crystal (triangles) coexistence densities, as well as  $\chi_{\text{max}}$  (diamonds). The inset is a schematic phase diagram for a polymer-colloid mixture with size ratio  $q = 0.6$ , taken from Ref. [7].

phase diagram is shown in Fig. 1 as a function of the bulk density  $\rho_b$  and either the mean swim speed  $v_b$  (a) or the free swim speed  $s$  (b), as expressed in scaled form by the Péclet number  $\text{Pe} = s \sigma \gamma / (k_B T)$ . The topology of the phase diagram matches that obtained in simulation work [14,15] and the reasonable agreement with the simulation results by Turci and Wilding [14] is very satisfactory; their results for the phase diagram are displayed in Fig 1(c). Our theory reproduces the

marginal stability [15] of active gas-liquid coexistence with respect to freezing into a dense fcc crystal. The coexisting gas has relatively high density, in stark contrast to the strong dilution of the coexisting gas that occurs quickly in equilibrium phase separation when moving away from the triple point.

On the basis of the similarity of their simulation results for the active system to depletion-induced phase behavior in equilibrium [comparing the main plot and inset of Fig. 1(c)], Turci and Wilding [14] draw conclusions about the presence and relevance of effective many-body interactions that govern the active system. While it is well-established that in active systems the Péclet number plays a role similar to that of temperature in equilibrium, the proposal by Turci and Wilding leaves open whether one should think of the activity as only generating many-body effects that are akin to those of depletants or whether the active system contains actual degrees of freedom that have not been properly appreciated.

Based on the success of our theory, we argue that the latter is the case and that, besides the density, the velocity field is an intrinsic degree of freedom that the nonequilibrium system can regulate freely and self-consistently. To demonstrate the validity of this concept, we use the actual mean velocity  $v_b$  instead of  $Pe$  as a state variable in Fig. 1(a). The swim speed  $v_b$  is high in the coexisting gas, low in the coexisting liquid, and even lower in the coexisting crystal. The latter property is consistent with Caprini *et al.* reporting very low swim speeds in solid clusters of the two-dimensional ABP system, see the Supplemental Material of Ref. [61]. This behavior is analogous to what is found in depletion-driven phase separation, when going from the reservoir density of the depletant to the actual depletant density in the system [7,8]. The observed similarity in the form of the phase diagram is striking, compare the main plot and the inset of Fig. 1(a).

We next investigate whether our proposed theory is predictive beyond the phase diagram. In their simulation work [14], Turci and Wilding have investigated the statistics of particle number fluctuations, as they occur in small virtual subboxes of the global system. The strength of fluctuations  $\chi(\rho_b)$  is taken to be a proxy for the compressibility, as can, in equilibrium, be obtained from the thermodynamical derivative  $\partial\rho_b(\mu)/\partial\mu$ , carried out in the grand ensemble where global particle number fluctuations occur. These fluctuations are absent in the present system, as the particle number is conserved in time [we recall the validity of even the locally resolved continuity equation (1)].

Within our nonequilibrium framework, the partial derivative  $\chi(\mu_b) = \partial\rho_b(\mu)/\partial\mu$  is well-defined. Here  $\mu$  is the total chemical potential and we recall its splitting (6) into adiabatic and superadiabatic contributions. We invert via  $\chi(\mu_b) = [\partial\mu(\rho_b)/\partial\rho_b]^{-1}$  with the derivative taken at  $T, Pe = \text{const.}$  We normalize with respect to the low density behavior,  $\chi(\rho_b)/\chi(0)$ , as has also been done in the simulations [14]. To create further common ground, we scale the density axis by the respective value of the critical density  $\rho_c$ . From the setup of the theory, we expect  $\chi(\rho_b)/\chi(0)$  to be a measure of particle fluctuations and we show numerical results in Fig. 2(a) as a function of  $\rho_b/\rho_c$  for a range of different values of  $Pe/Pe_c < 1$ , where  $Pe_c$  indicates the critical value of the Péclet number. We find that the theory produces the same bell-shaped variation upon increasing density at fixed  $Pe$ , as is

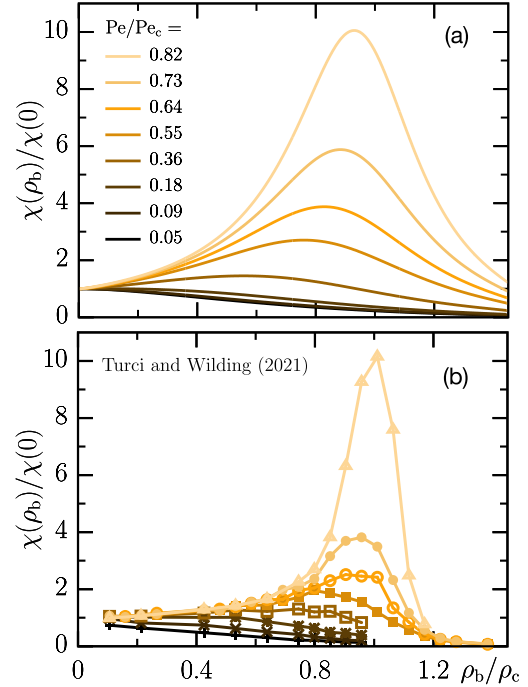


FIG. 2. Scaled compressibility  $\chi(\rho_b)/\chi(0)$  as a function of the scaled bulk density  $\rho_b/\rho_c$ , where  $\rho_c$  is the density at the MIPS critical point and  $\chi(0)$  is the low-density limit of the compressibility. The theoretical results in (a) are obtained from differentiating  $\chi(\rho_b) = \partial\rho(\mu)/\partial\mu|_{T,Pe}$ , where  $\mu$  is the (total) nonequilibrium chemical potential. Results are shown for a sequence of Péclet numbers (as indicated), scaled by the value at the critical point. (b) Corresponding simulation results of Ref. [14]; for the purpose of this comparison, we take  $Pe_c = 36$ ,  $\rho_c = 0.94$  in simulation [14] and  $Pe_c = 37.6$ ,  $\rho_c = 0.71$  for the theory. The lines in (b) connect the data points to guide the eye.

apparent in the simulation results reproduced in Fig. 2(b). The maximum becomes much more pronounced upon increasing  $Pe/Pe_c$  and the theoretical prediction consistently diverges at the nonequilibrium critical point. The position of the maximum of  $\chi(\rho_b)/\chi(0)$  traces a line in the phase diagram. The result is shown in Fig. 1, which again agrees very well with the simulation data [compare the orange line in Fig. 1(b) with the orange symbols in panel in Fig. 1(c)].

We take this satisfactory agreement of the simulation results [14] for particle number fluctuations against an analogous parametric derivative of our nonequilibrium state function as a test of the intrinsic consistency of our treatment. The theory, in particular, reproduces the strong increase in measured particle number fluctuations near the nonequilibrium critical point. As we derive nonequilibrium phase coexistence from the same state function, we conclude that our approach indeed captures much of the essence of the nonequilibrium statistical physics under consideration. We recall that we obtain the bulk pressure  $P(\rho_b)$  via integrating the identity  $\rho_b \partial\mu(\rho_b)/\partial\rho_b = \partial P(\rho_b)/\partial\rho_b$ , which implies mechanical stability in our formulation of the nonequilibrium physics [45–47]. The investigation of the particle number fluctuations, as measured via  $\chi(\rho_b)$ , provides a test for the validity of the source material on the left-hand side of the

equation, as  $\rho_b \partial \mu(\rho_b) / \partial \rho_b = \rho_b / \chi(\mu_b)$ . To shed further light on the particle number fluctuation problem, given the prominent role that the Ornstein-Zernike theory plays in describing fluctuations in equilibrium [1], we can imagine that concepts of the nonequilibrium Ornstein-Zernike framework [62,63] could pave a way forward.

In summary, we have investigated the nonequilibrium phase behavior of ABPs in three dimensions based on power functional concepts. The central assumption is that the formally exact nonequilibrium force balance relationship contains a nonequilibrium structural force contribution, as obtained by the negative spatial gradient of a corresponding superadiabatic chemical potential, Eq. (8). We have shown that the theory predicts the phase diagram correctly and that nonequilibrium particle number fluctuations are described in agreement with the observations in simulations. We envisage that going beyond the simple cell theory for the description of the crystal is possible with classical density functional theory [64] based on fundamental measure theory [2,28] as used to study the direct correlation function in crystals [65]. Given the recent progress in measurement of intercolloidal forces in gel states [66], it does not seem inconceivable that experiments can shed further light on active forces.

In our present treatment, we have characterized the steady-state one-body velocity field  $\mathbf{v}(\mathbf{r}, \boldsymbol{\omega})$  in each of the three nonequilibrium phases by the value of the mean swim speed  $v_b$ . For both the active gas and the active liquid phase, due to their rotational and translational invariances,  $v_b = \mathbf{v}(\mathbf{r}, \boldsymbol{\omega}) \cdot \boldsymbol{\omega}$  indeed becomes independent of position  $\mathbf{r}$  and of orientation  $\boldsymbol{\omega}$ . Thus, the full information is retained and the velocity field is  $\mathbf{v}(\mathbf{r}, \boldsymbol{\omega}) = v_b \boldsymbol{\omega}$  for active bulk fluids. We also describe the crystal on the basis of the single parameter  $v_b$ , which we take to be a coarse-grained and global measure of the activity across the spatial inhomogeneity of the lattice. It thus remains to study and describe fully the inhomogeneous flow field in the crystal,  $\mathbf{v}(\mathbf{r}, \boldsymbol{\omega})$ , which we deem to be an interesting problem, not least in the light of the velocity-alignment effects identified by Caprini *et al.* in two dimensions [61].

Recently, Evans and Omar [67] addressed active freezing theoretically. Furthermore, an experimental investigation of freezing of passive colloids in an active solvent was reported by Massana-Cid *et al.* [68]. It would be interesting to relate to these studies in future work.

We thank F. Turci for sending us the simulation data of Ref. [14] and himself, N. Wilding, and D. de las Heras for useful and inspiring discussions.

- 
- [1] J. P. Hansen and I. R. McDonald, *Theory of Simple Liquids*, 4th ed. (Academic Press, London, 2013).
- [2] P. Tarazona, Density functional for hard sphere crystals: A fundamental measure approach, *Phys. Rev. Lett.* **84**, 694 (2000).
- [3] M. E. Leunissen, C. G. Christova, A.-P. Hynninen, C. P. Royall, A. I. Campbell, A. Imhof, M. Dijkstra, R. van Roij, and A. van Blaaderen, Ionic colloidal crystals of oppositely charged particles, *Nature (London)* **437**, 235 (2005).
- [4] T. Hueckel, G. M. Hocky, J. Palacci, and S. Sacanna, Ionic solids from common colloids, *Nature (London)* **580**, 487 (2020).
- [5] C. N. Likos, Effective interactions in soft condensed matter physics, *Phys. Rep.* **348**, 267 (2001).
- [6] R. Tuinier, J. Rieger, and C. G. de Kruif, Depletion-induced phase separation in colloid-polymer mixtures, *Adv. Colloid Interface Sci.* **103**, 1 (2003).
- [7] M. Dijkstra, J. M. Brader, and R. Evans, Phase behaviour and structure of model colloid-polymer mixtures, *J. Phys.: Condens. Matter* **11**, 10079 (1999).
- [8] M. Schmidt, H. Löwen, J. M. Brader, and R. Evans, Density functional for a model colloid-polymer mixture, *Phys. Rev. Lett.* **85**, 1934 (2000).
- [9] S. L. Taylor, R. Evans, and C. P. Royall, Temperature as an external field for colloid-polymer mixtures: ‘quenching’ by heating and ‘melting’ by cooling, *J. Phys.: Condens. Matter* **24**, 464128 (2012).
- [10] K. Binder, P. Virnau, and A. Statt, Perspective: the Asakura Oosawa model: A colloid prototype for bulk and interfacial phase behavior, *J. Chem. Phys.* **141**, 559 (2014).
- [11] K. Miyazaki, K. S. Schweizer, D. Thirumalai, R. Tuinier, and E. Zaccarelli, The Asakura-Oosawa theory: Entropic forces in physics, biology, and soft matter, *J. Chem. Phys.* **156**, 080401 (2022).
- [12] G. Campos-Villalobos, E. Boattini, L. Filion, and M. Dijkstra, Machine learning many-body potentials for colloidal systems, *J. Chem. Phys.* **155**, 174902 (2021).
- [13] G. Campos-Villalobos, G. Giunta, S. Marín-Aguilar, and M. Dijkstra, Machine-learning effective many-body potentials for anisotropic particles using orientation-dependent symmetry functions, *J. Chem. Phys.* **157**, 024902 (2022).
- [14] F. Turci and N. B. Wilding, Phase separation and multibody effects in three-dimensional active Brownian particles, *Phys. Rev. Lett.* **126**, 038002 (2021).
- [15] A. K. Omar, K. Klymko, T. GrandPre, and P. L. Geissler, Phase diagram of active Brownian spheres: Crystallization and the metastability of motility-induced phase separation, *Phys. Rev. Lett.* **126**, 188002 (2021).
- [16] J. Bialké, T. Speck, and H. Löwen, Crystallization in a dense suspension of self-propelled particles, *Phys. Rev. Lett.* **108**, 168301 (2012).
- [17] A. Wysocki, R. G. Winkler, and G. Gompper, Cooperative motion of active Brownian spheres in three-dimensional dense suspensions, *Europhys. Lett.* **105**, 48004 (2014).
- [18] F. J. Moore, C. P. Royall, T. B. Liverpool, and J. Russo, Crystallisation and polymorph selection in active Brownian particles, *Eur. Phys. J. E* **44**, 121 (2021).
- [19] S. Paliwal, J. Rodenburg, R. van Roij, and M. Dijkstra, Chemical potential in active systems: Predicting phase equilibrium from bulk equations of state? *New J. Phys.* **20**, 015003 (2018).
- [20] A. P. Solon, J. Stenhammar, M. E. Cates, Y. Kafri, and J. Tailleur, Generalized thermodynamics of phase equilibria in scalar active matter, *Phys. Rev. E* **97**, 020602(R) (2018).
- [21] T. Speck, Coexistence of active Brownian disks: Van der Waals theory and analytical results, *Phys. Rev. E* **103**, 012607 (2021).
- [22] T. Speck, Critical behavior of active Brownian particles: Connection to field theories, *Phys. Rev. E* **105**, 064601 (2022).

- [23] J. Bickmann and R. Wittkowski, Predictive local field theory for interacting active Brownian spheres in two spatial dimensions, *J. Phys.: Condens. Matter* **32**, 214001 (2020).
- [24] A. K. Omar, H. Row, S. A. Mallory, and J. F. Brady, Mechanical theory of nonequilibrium coexistence and motility-induced phase separation, *Proc. Natl. Acad. Sci. USA* **120**, e2219900120 (2023).
- [25] G. Szamel, Theory for the dynamics of dense systems of athermal self-propelled particles, *Phys. Rev. E* **93**, 012603 (2016).
- [26] R. Evans, The nature of the liquid-vapour interface and other topics in the statistical mechanics of non-uniform, classical fluids, *Adv. Phys.* **28**, 143 (1979).
- [27] R. Evans, M. Oettel, R. Roth, and G. Kahl, New developments in classical density functional theory, *J. Phys.: Condens. Matter* **28**, 240401 (2016).
- [28] R. Roth, Fundamental measure theory for hard-sphere mixtures: A review, *J. Phys.: Condens. Matter* **22**, 063102 (2010).
- [29] A. Mauleon-Amieva, M. Mosayebi, J. E. Hallett, F. Turci, T. B. Liverpool, J. S. van Duijneveldt, and C. P. Royall, Competing active and passive interactions drive amoebalike crystallites and ordered bands in active colloids, *Phys. Rev. E* **102**, 032609 (2020).
- [30] J. Palacci, S. Sacanna, A. P. Steinberg, D. J. Pine, and P. M. Chaikin, Living crystals of light-activated colloidal surfers, *Science* **339**, 936 (2013).
- [31] N. A. Söker, S. Auschra, V. Holubec, K. Kroy and F. Cichos, How activity landscapes polarize microswimmers without alignment forces, *Phys. Rev. Lett.* **126**, 228001 (2021).
- [32] S. Auschra, V. Holubec, N. A. Söker, F. Cichos, and K. Kroy, Polarization-density patterns of active particles in motility gradients, *Phys. Rev. E* **103**, 062601 (2021).
- [33] F. Kümmel, P. Shabestari, C. Lozano, G. Volpe, and C. Bechinger, Formation, compression and surface melting of colloidal clusters by active particles, *Soft Matter* **11**, 6187 (2015).
- [34] F. Ginot, A. Solon, Y. Kafri, C. Ybert, J. Tailleur and C. Cottin-Bizonne, Sedimentation of self-propelled Janus colloids: Polarization and pressure, *New J. Phys.* **20**, 115001 (2018).
- [35] A. F. Carreira, A. Wysocki, C. Ybert, M. Leocmach, H. Rieger, C. Cottin-Bizonne, How to steer active colloids up a vertical wall, [arXiv:2307.02810](https://arxiv.org/abs/2307.02810).
- [36] N. Klongvessa, F. Ginot, C. Ybert, C. Cottin-Bizonne, and M. Leocmach, Nonmonotonic behavior in dense assemblies of active colloids, *Phys. Rev. E* **100**, 062603 (2019).
- [37] F. Turci and N. B. Wilding, Wetting transition of active Brownian particles on a thin membrane, *Phys. Rev. Lett.* **127**, 238002 (2021).
- [38] M. James, D. A. Suchla, J. Dunkel, and M. Wilczek, Emergence and melting of active vortex crystals, *Nat. Commun.* **12**, 5630 (2021).
- [39] C. M. Koch and M. Wilczek, Role of advective inertia in active nematic turbulence, *Phys. Rev. Lett.* **127**, 268005 (2021).
- [40] E. Chacón, F. Alarcón, J. Ramirez, P. Tarazona, and C. Valeriani, Intrinsic structure perspective for MIPS interfaces in two-dimensional systems of active Brownian particles, *Soft Matter* **18**, 2646 (2022).
- [41] J. Martín-Roca, R. Martínez, L. C. Alexander, A. L. Diez, D. G. A. L. Aarts, F. Alarcon, J. Ramírez, and C. Valeriani, Characterization of MIPS in a suspension of repulsive active Brownian particles through dynamical features, *J. Chem. Phys.* **154**, 164901 (2021).
- [42] M. Schmidt, Power functional theory for many-body dynamics, *Rev. Mod. Phys.* **94**, 015007 (2022).
- [43] P. Krinninger, M. Schmidt, and J. M. Brader, Nonequilibrium phase behaviour from minimization of free power dissipation, *Phys. Rev. Lett.* **117**, 208003 (2016).
- [44] P. Krinninger and M. Schmidt, Power functional theory for active Brownian particles: General formulation and power sum rules, *J. Chem. Phys.* **150**, 074112 (2019).
- [45] S. Hermann, D. de las Heras, and M. Schmidt, Phase separation of active Brownian particles in two dimensions: Anything for a quiet life, *Mol. Phys.* **119**e1902585 (2021).
- [46] S. Hermann, P. Krinninger, D. de las Heras, and M. Schmidt, Phase coexistence of active Brownian particles, *Phys. Rev. E* **100**, 052604 (2019).
- [47] S. Hermann, D. de las Heras, and M. Schmidt, Non-negative interfacial tension in phase-separated active Brownian particles, *Phys. Rev. Lett.* **123**, 268002 (2019).
- [48] S. Hermann and M. Schmidt, Noether's theorem in statistical mechanics, *Commun. Phys.* **4**, 176 (2021).
- [49] F. Sammüller, S. Hermann, D. de las Heras, and M. Schmidt, Noether-constrained correlations in equilibrium liquids, *Phys. Rev. Lett.* **130**, 268203 (2023).
- [50] S. Hermann and M. Schmidt, Active interface polarization as a state function, *Phys. Rev. Res.* **2**, 022003(R) (2020).
- [51] D. de las Heras, T. Zimmermann, F. Sammüller, S. Hermann and M. Schmidt, Perspective: How to overcome dynamical density functional theory, *J. Phys.: Condens. Matter* **35**, 271501 (2023).
- [52] F. Sammüller, S. Hermann, D. de las Heras, and M. Schmidt, Neural functional theory for inhomogeneous fluids: Fundamentals and applications, *Proc. Natl. Acad. Sci. USA* **120**, e2312484120 (2023).
- [53] F. Sammüller, S. Hermann, and M. Schmidt, Why neural functionals suit statistical mechanics, [arXiv:2312.04681](https://arxiv.org/abs/2312.04681).
- [54] D. de las Heras and M. Schmidt, Flow and structure in nonequilibrium Brownian many-body systems, *Phys. Rev. Lett.* **125**, 018001 (2020).
- [55] R. van Damme, J. Rodenburg, R. van Roij, and M. Dijkstra, Interparticle torques suppress motility-induced phase separation for rodlike particles, *J. Chem. Phys.* **150**, 164501 (2019).
- [56] P. Paricaud, Extension of the BMCSL equation of state for hard spheres to the metastable disordered region: Application to the SAFT approach, *J. Chem. Phys.* **143**, 044507 (2015).
- [57] W. G. Hoover and F. H. Ree, Use of computer experiments to locate the melting transition and calculate the entropy in the solid phase, *J. Chem. Phys.* **47**, 4873 (1967).
- [58] W. G. Hoover and F. H. Ree, Melting transition and communal entropy for hard spheres, *J. Chem. Phys.* **49**, 3609 (1968).
- [59] D. Frenkel and A. J. C. Ladd, New Monte Carlo method to compute the free energy of arbitrary solids. Application to the fcc and hcp phases of hard spheres, *J. Chem. Phys.* **81**, 3188 (1984).
- [60] C. P. Royall, P. Charbonneau, M. Dijkstra, J. Russo, F. Smallenburg, T. Speck, and C. Valeriani, Colloidal Hard Spheres: Triumphs, challenges and mysteries, [arXiv:2305.02452](https://arxiv.org/abs/2305.02452).

- [61] L. Caprini, U. Marini Bettolo Marconi, and A. Puglisi, Spontaneous velocity alignment in motility-induced phase separation, *Phys. Rev. Lett.* **124**, 078001 (2020).
- [62] J. M. Brader and M. Schmidt, Dynamic correlations in Brownian many-body systems, *J. Chem. Phys.* **140**, 034104 (2014).
- [63] J. M. Brader and M. Schmidt, Nonequilibrium Ornstein-Zernike relation for Brownian many-body dynamics, *J. Chem. Phys.* **139**, 104108 (2013).
- [64] J. M. Häring, C. Walz, G. Szamel, and M. Fuchs, Coarse-grained density and compressibility of nonideal crystals: General theory and an application to cluster crystals, *Phys. Rev. B* **92**, 184103 (2015).
- [65] S.-C. Lin, M. Oettel, J. M. Häring, R. Haussmann, M. Fuchs, and G. Kahl, Direct correlation function of a crystalline solid, *Phys. Rev. Lett.* **127**, 085501 (2021).
- [66] J. Dong, F. Turci, R. L. Jack, M. A. Faers, and C. P. Royall, Direct imaging of contacts and forces in colloidal gels, *J. Chem. Phys.* **156**, 214907 (2022).
- [67] D. Evans and A. K. Omar, Theory of nonequilibrium symmetry-breaking coexistence and active crystallization, [arXiv:2309.10341](https://arxiv.org/abs/2309.10341).
- [68] H. Massana-Cid, C. Maggi, N. Gnan, G. Frangipane, R. Di Leonardo, Multiple temperatures and melting of a colloidal active crystal, [arXiv:2401.09911](https://arxiv.org/abs/2401.09911).